

Catalytic asymmetric addition of an amine N–H bond across internal alkenes

<https://doi.org/10.1038/s41586-020-2919-z>

Yumeng Xi^{1,2}, Senjie Ma^{1,2} & John F. Hartwig^{1,2}✉

Received: 26 November 2019

Accepted: 27 October 2020

Published online: 03 November 2020

 Check for updates

Hydroamination of alkenes, the addition of the N–H bond of an amine across an alkene, is a fundamental, yet challenging, organic transformation that creates an alkylamine from two abundant chemical feedstocks, alkenes and amines, with full atom economy^{1–3}. The reaction is particularly important because amines, especially chiral amines, are prevalent substructures in a wide range of natural products and drugs. Although extensive efforts have been dedicated to developing catalysts for hydroamination, the vast majority of alkenes that undergo intermolecular hydroamination have been limited to conjugated, strained, or terminal alkenes^{2–4}; only a few examples occur by the direct addition of the N–H bond of amines across unactivated internal alkenes^{5–7}, including photocatalytic hydroamination^{8,9}, and no asymmetric intermolecular additions to such alkenes are known. In fact, current examples of direct, enantioselective intermolecular hydroamination of any type of unactivated alkene lacking a directing group occur with only moderate enantioselectivity^{10–13}. Here we report a cationic iridium system that catalyses intermolecular hydroamination of a range of unactivated, internal alkenes, including those in both acyclic and cyclic alkenes, to afford chiral amines with high enantioselectivity. The catalyst contains a phosphine ligand bearing trimethylsilyl-substituted aryl groups and a triflimide counteranion, and the reaction design includes 2-amino-6-methylpyridine as the amine to enhance the rates of multiple steps within the catalytic cycle while serving as an ammonia surrogate. These design principles point the way to the addition of N–H bonds of other reagents, as well as O–H and C–H bonds, across unactivated internal alkenes to streamline the synthesis of functional molecules from basic feedstocks.

Chiral amines are essential structural motifs in numerous active pharmaceutical ingredients and in many agrochemicals and materials. They also serve as chiral catalysts, resolving reagents and chiral auxiliaries¹⁴. Thus, efficient methods to prepare chiral amines have been long sought. Traditional approaches¹⁵ include chemical^{16,17} and enzymatic¹⁸ reductive amination, hydrogenation¹⁹, nucleophilic addition to imines²⁰ and nucleophilic substitution^{21,22}. However, these methods require starting materials containing reactive functionality that is often derived from feedstock alkenes. Thus, hydroamination of alkenes is the most direct method to construct chiral amines from a functional group that is present in basic feedstocks and is typically unprotected. Asymmetric additions to conjugated alkenes, such as dienes^{23–26} and vinylarenes^{27,28}, have been reported, but the scope of the direct addition of N–H bonds to more common and less reactive unconjugated alkenes is severely limited, and the enantioselectivities of asymmetric processes are far lower than those that would enable applications for the synthesis of chiral amines. Formal hydroaminations provide an alternative approach to this problem, but the use of silanes with electrophilic aminating reagents²⁹ and even metal reductants³⁰, instead of amines, undermines the atom economy of the hydroamination reaction. Direct N–H additions of unactivated internal alkenes that occur with high enantioselectivity are unknown.

There are considerable challenges facing the development of catalytic hydroaminations of unactivated alkenes that bear more than one substituent (Fig. 1a). Both experiments and theoretical studies have shown that the thermodynamic driving force is weak and the kinetic barrier to combining two nucleophiles is high^{1,31}. Moreover, catalysts for hydroamination often catalyse undesirable, competing alkene isomerization, and isomerization is typically faster than addition of the N–H bond during many metal-catalysed hydroaminations (Fig. 1b). Such relative rates lead to a mixture of isomeric products^{32,33}. Many catalysts for alkene hydroamination also promote formation of oxidative amination products by β -hydrogen elimination of β -aminoalkylmetal intermediates^{34,35}. These isomerization and oxidative side reactions must be suppressed to achieve hydroamination of unactivated internal alkenes. Finally, because hydroamination is usually almost ergoneutral, isomerization and racemization of the products during the reaction can erode regioselectivity and enantioselectivity³⁶.

To address these challenges, we modified a neutral iridium complex containing a bisphosphine ligand, which was previously shown to catalyse the formation of hydroamination and oxidative amination products from the reaction of terminal alkenes with amides and indoles^{34,37–40}. We have previously shown that these aminations occur by a mechanism

¹Department of Chemistry, University of California, Berkeley, CA, USA. ²Division of Chemical Sciences, Lawrence Berkeley National Laboratory, Berkeley, CA, USA. ✉e-mail: jhartwig@berkeley.edu

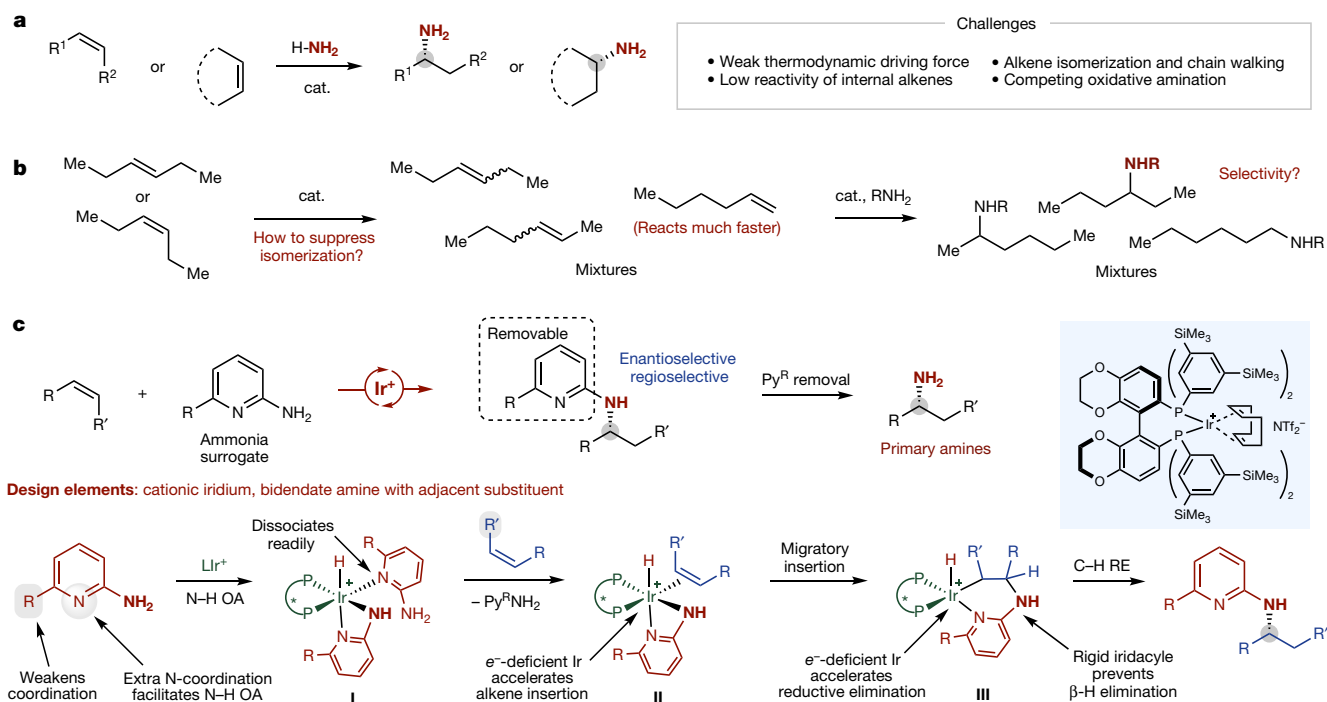


Fig. 1 | Catalytic asymmetric hydroamination of unactivated internal alkenes. **a**, Long-standing challenges and previous strategies for catalytic hydroamination of unactivated internal alkenes. **b**, Alkene isomerization that leads to a mixture of constitutional isomeric products. **c**, Design of a cationic

iridium catalyst and an ammonia surrogate based on 2-aminopyridine to achieve asymmetric hydroamination of internal alkenes. OA, oxidative addition. RE, reductive elimination.

comprising oxidative addition of N–H bonds, migratory insertion of alkenes and reductive elimination of C–H bonds³⁴. We envisioned that switching the iridium catalyst from neutral to cationic would lead to the formation of cationic iridium intermediates that would undergo migratory insertion of the alkene more rapidly⁴¹, a step that has been shown to be rate-limiting in the reaction of terminal alkenes with the neutral catalyst³⁴ (Fig. 1c). If binding and insertion of the alkene were sufficiently enhanced, then the reaction scope might include internal alkenes. In addition, we envisioned that coordinating groups adjacent to the amine (for example, 2-aminopyridine derivatives) could facilitate and make more thermodynamically favourable the initial N–H oxidative addition, and such enhancements of this step could be important because the rate of oxidative addition of electron-deficient metal complexes is generally slower than that of electron-rich ones⁴². If properly placed, the coordinating groups of the amine could also form a rigid six-membered iridacycle upon insertion of the alkene; this geometry could suppress β -hydrogen elimination to form enamines. Such a combination of 2-aminopyridine and a cationic iridium catalyst was evaluated¹² for the hydroamination of terminal vinylarenes, but only briefly for the hydroamination of unactivated α -alkenes. Low enantioselectivities ($\leq 11\%$ enantiomeric excess, e.e.) were observed, and the reactions of unstrained internal alkenes were not examined. We reasoned that a substituent near the binding group of the amine could modulate the strength of the coordination of the pyridine, leading to potential enhancement of the activity of the iridium catalyst, due to weakened coordination (Fig. 1c). Finally, the pyridyl group of the product could be cleaved by known methods to reveal the corresponding primary amine⁴³.

Figure 2 summarizes our studies on the development of a cationic iridium catalyst and an ammonia surrogate for the asymmetric hydroamination of unactivated internal alkenes. These experiments revealed the effect of the reaction components of the system on the reaction yield, level of alkene isomerization and enantioselectivity. To identify a suitable ammonia surrogate for this reaction, we surveyed

a series of heteroaromatic amines and one control arylamine that possess varying structural properties. The hydroamination products from these reactions consisted of three isomers (denoted **A**, **B** and **C**) that probably resulted from competing alkene isomerization and hydroamination. A larger amount of **A** reflects a faster rate for direct addition of the amine to the starting alkene than alkene isomerization before addition.

As shown in Fig. 2a, hydroamination of *cis*-4-octene in the presence of $[Ir(\text{coe})_2\text{Cl}]_2$, (*S*)-DTBM-SEGPPOS ((*S*)-(+)-5,5'-bis[di(3,5-*tert*-butyl-4-methoxyphenyl)phosphino]-4,4'-bi-1,3-benzodioxole) and NaBARF (sodium tetrakis[3,5-bis(trifluoromethyl)phenyl]borate) occurred only when 6-substituted 2-aminopyridine derivatives were used as the amine source. The hydroamination of 2-amino-6-methylpyridine formed amines **A**, **B** and **C** in a combined 73% yield, with **A** constituting 28% of the amine products (defined as $A/(A+B+C)$). The reaction of 2-amino-6-trifluoromethylpyridine afforded only 5% of isomer **A**. Other amines tested, including the parent 2-aminopyridine, did not undergo this hydroamination. These results suggest that the substituent in the 6-position of the pyridine ring is essential to promote the hydroamination.

To suppress competing alkene isomerization and improve the reaction yield, we examined catalysts containing a series of bisphosphine ligands and counteranions for hydroamination with 2-amino-6-methylpyridine as the amine. Studies of the electronic and steric properties of ligands indicated that the ligands that are less electron-rich (Fig. 2b, entry 2) and more sterically encumbered (Fig. 2b, entries 3–5) than (*S*)-DTBM-SEGPPOS form catalysts that are more reactive and selective for direct addition to form amine **1**. The observed higher reactivity of catalysts generated from more electron-poor ligands probably results from a greater rate of migratory insertion of the alkene (see below) into the Ir–N bond of complexes containing **L2–L5** lacking the methoxy group than into the Ir–N bond of the complex ligated by (*S*)-DTBM-SEGPPOS possessing the *p*-OMe group⁴⁴. The higher selectivity from the more hindered ligands could

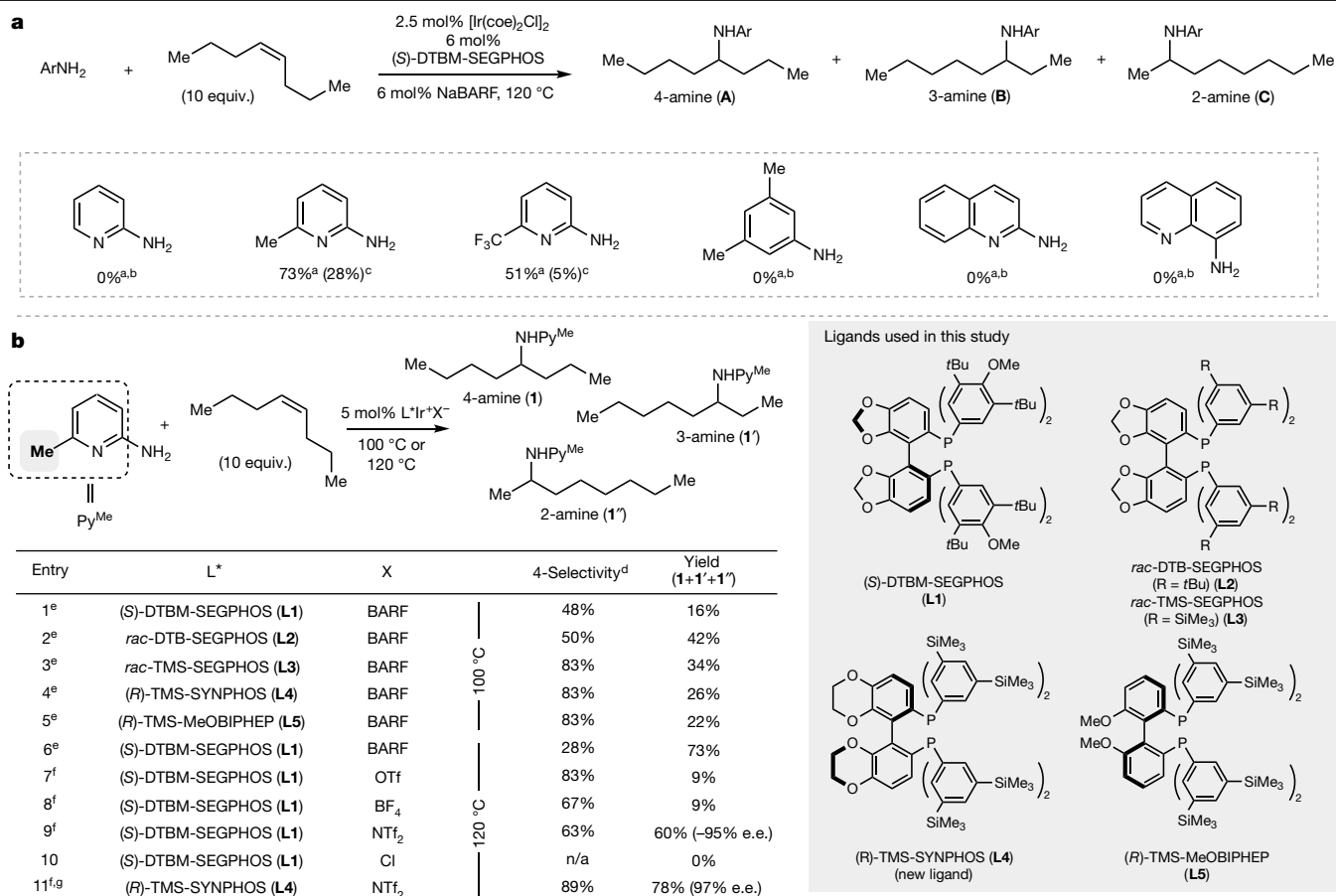


Fig. 2 | Development of asymmetric hydroamination of unactivated internal alkenes with 2-amino-6-methylpyridine as an ammonia surrogate.

a, Identification of suitable ammonia surrogates to enable hydroamination of unactivated internal alkenes. **b**, Identification of reaction conditions to achieve asymmetric hydroamination and to suppress alkene

result from a greater sensitivity of the rate of insertion of the alkene into the metal–amido bond (Fig. 1c, structure II) to steric effects than the rate of insertion into the metal–hydride bond, which probably leads to alkene isomerization^{45,46}. Studies with various counterions revealed that reactions with triflimide as the counterion of the catalyst occurred with the highest selectivity at high conversion (Fig. 2b, entries 6–9). The origin of the effects of the counterions is difficult to ascertain, but an effect is clear. Control experiments showed that the reaction catalysed by a neutral iridium complex under otherwise identical conditions (Fig. 2b, entry 10) resulted in the exclusive formation of oxidative amination products. By combining the chiral ligand that led to the highest selectivity with the triflimide anion in the form of [((*R*)-TMS-SYNPHOS)Ir(COD)]NTf₂, the model hydroamination reaction formed the 4-amino-octane (1) in high yield; this reaction also occurred with remarkably high enantioselectivity (Fig. 2b, entry 11). Thus, the substituent on the amine, the new phosphine ligand and the use of a triflimide counterion all led to the high activity, chemoselectivity and enantioselectivity of the reaction.

With this catalyst and reagent, we examined the scope of alkenes that underwent hydroamination (Fig. 3). Both symmetrical internal alkenes and unsymmetrical internal alkenes underwent hydroamination with 2-amino-6-methylpyridine. The reactions all proceeded in greater than 90% e.e. Hydroamination of symmetrical alkenes afforded products containing linear alkyl groups (1), aryl-substituted alkyl groups (2), branched alkyl groups (3), silyloxy groups (4), alkoxy groups (5) and alkoxy-carbonyl groups (6) in good to high yields. Reactions of

isomerization. ^aCombined yield. ^bNo reaction. ^cDefined as $\mathbf{A}/(\mathbf{A} + \mathbf{B} + \mathbf{C})$. ^d4-Selectivity defined as $\mathbf{1}/(\mathbf{1} + \mathbf{1}' + \mathbf{1}'')$. ^eConditions: 2.5 mol% [Ir(coe)₂Cl]₂, 6 mol% ligand, 6 mol% NaBARF, toluene. ^fConditions: 5 mol% [L*Ir(COD)]X, toluene. ^gIn 2-MeTHF.

unsymmetrical internal alkenes bearing polar functional groups at the homoallylic position occurred with synthetically useful regioselectivity (2:1 to 10:1). These functional groups include phthalimidyl groups (7, 8), sulfonamido groups (9), silyloxy groups (10), bis(ethoxycarbonyl) methyl groups (11) and (hetero)aryloxy groups (12–14). These groups presumably influence the regioselectivity by inductive effects that are similar to those observed for other classes of functionalization of unsymmetrical internal alkenes^{47–49}.

The reactivity of the system for *Z*-alkenes enabled the hydroamination of cyclic alkenes, and these reactions also occurred with high enantioselectivity. The combination of [Ir(coe)₂Cl]₂, (S)-DTBM-SEGPHOS and NaBARF was used as the catalyst because it was more reactive than [((*R*)-TMS-SYNPHOS)Ir(COD)]NTf₂ for the hydroamination of cyclic alkenes. The cyclic hydrocarbons cyclopentene, cyclohexene, cycloheptene and cyclooctene all underwent hydroamination in high yields (15–18). The hydroamination of a series of substituted cyclopentenes formed chiral amine products with high enantioselectivity (19–23, 90–92% e.e.). The reaction to form the 1,3-substituted cyclopentane 23 from the 4-methoxycarbonyl-substituted cyclopentene occurred with high diastereoselectivity for the *trans* product. In addition, cyclohexene derivatives with 3,3-substituents underwent hydroamination to afford two products with regioselectivity of approximately 1:3 (24/24', 25/25'). Although the major isomer is achiral, the chiral minor isomer was formed with good to high enantioselectivity. We observed in some cases that the hydroaminations of substituted cycloalkenes with rings larger than that of cyclopentene occurred to high conversion, but were

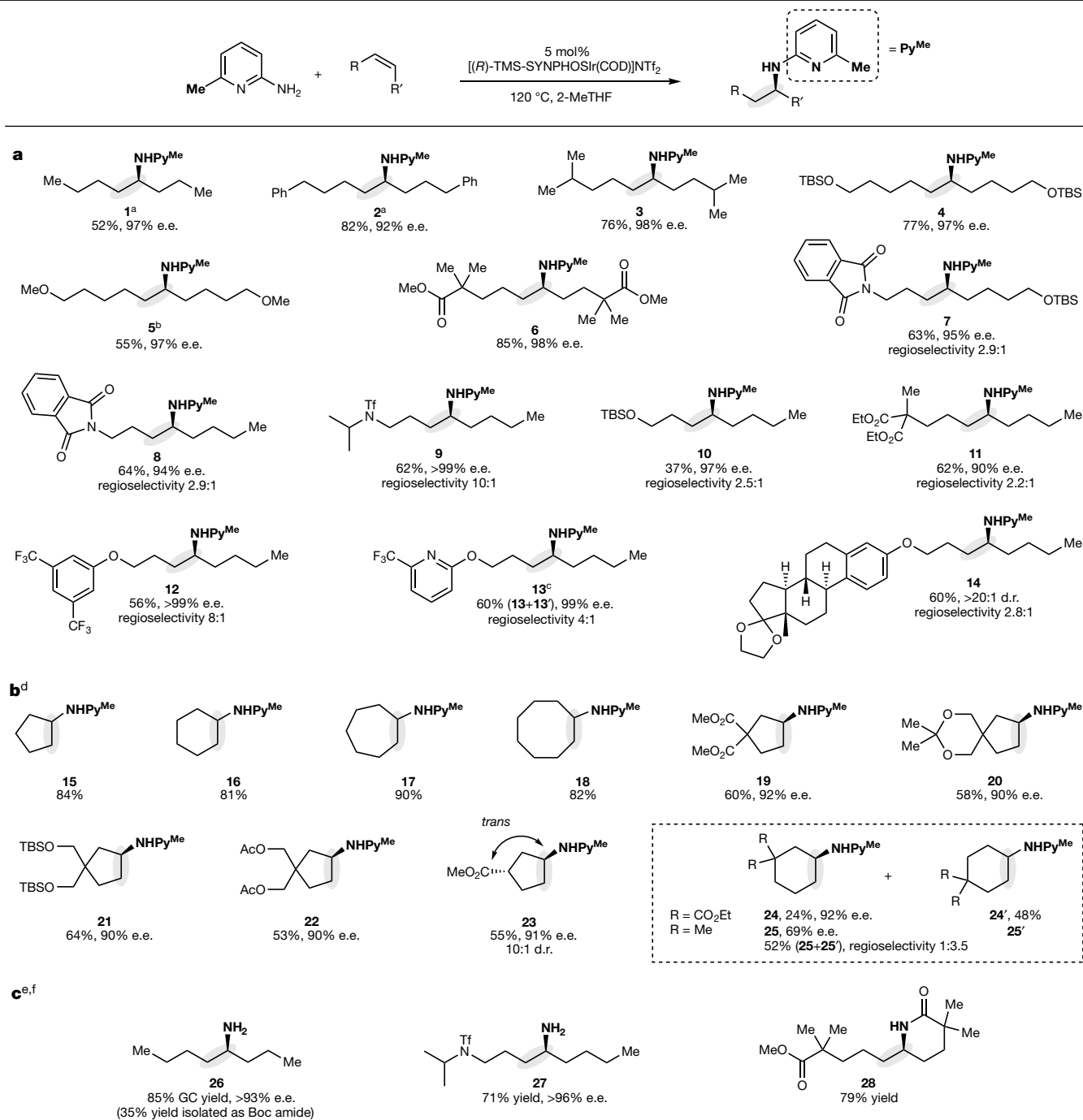


Fig. 3 | Scope of internal alkenes that undergo hydroamination. **a**, Scope of asymmetric hydroamination of acyclic internal alkenes. **b**, Scope of hydroamination of simple cycloalkenes and of asymmetric hydroamination of substituted cyclic alkenes. **c**, Products from the removal of the 2-(6-methyl)pyridyl group. ^a2.5 mol% catalyst. ^b7.5 mol% catalyst. ^c20 mol% catalyst.

^dConditions: 2.5 mol% [Ir(coe)₂Cl]₂, 7.5 mol% (*S*)-DTBM-SEGPHOS, 6 mol% NaBARF, 1,4-dioxane, 120 °C. ^eConditions: PtO₂, HCl, H₂ (1 atm); NaBH₄, THF/EtOH. ^fEnantioselectivities were determined after conversion to the original hydroamination product by palladium-catalysed cross-coupling of the primary amine with 2-bromo-6-methylpyridine.

complicated by competing alkene isomerization, which led to mixtures of isomers that were difficult to separate.

The pyridyl group of the hydroamination products (**1**, **9**) was cleaved by a short sequence that consisted of protonation, hydrogenation and borohydride reduction. The corresponding primary amines (**26**, **27**) formed in 71–85% yield with little or no erosion in enantiomeric excess (see Supplementary Information sections VI and X). By the same sequence, hydroamination product **6** was converted to the corresponding δ -lactam (**28**) in 79% yield.

To understand how the combination of a cationic iridium catalyst and 2-amino-6-methylpyridine enabled the hydroamination of unactivated internal alkenes, we investigated the reaction mechanism. The reaction of a substituted cyclopentene with *N,N*-dideuterio-2-amino-6-methylpyridine showed that the addition occurred in a *syn* fashion. This stereochemistry is consistent with a mechanism that involves migratory insertion of an alkene, rather than nucleophilic attack on a metal-bound alkene complex (Fig. 4a). Kinetic experiments showed that the reaction is first-order in

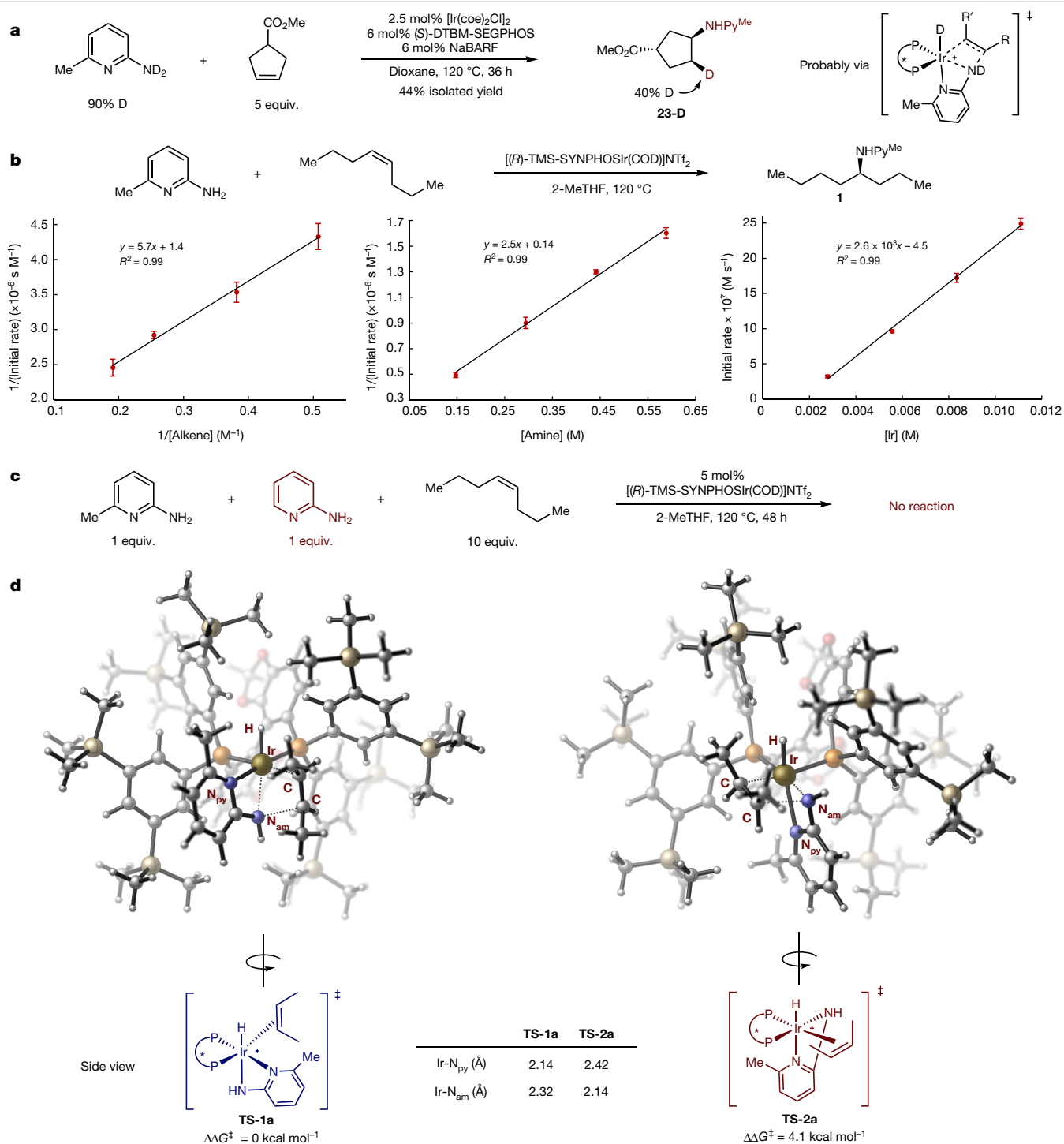


Fig. 4 | Mechanistic study of the hydroamination. **a**, Deuterium-labelling experiments. **b**, Experiments to reveal kinetic orders of each reaction component. **c**, Competition experiments using 2-amino-6-methylpyridine and 2-aminopyridine. **d**, Transition-state structures of alkene migratory insertion computed by DFT. Single-point energies were computed at the M06/6-311+G(d,p)/SDD/SMD(1,4-dioxane) level of theory with structures optimized at the B3LYP/6-31G(d)/SDD level. The ligand used for the calculations is

[iridium catalyst], positive-order in [*cis*-4-octene] and inverse-order in [2-amino-6-methylpyridine] (Fig. 4b). These data suggest that a molecule of 2-amino-6-methylpyridine dissociates reversibly from iridium in the catalyst resting state before rate-limiting insertion of the alkene, presumably into the metal–amido bond⁴¹. To elucidate why the methyl group of 2-amino-6-methylpyridine is essential in this

(*S*)-TMS-SEGPHOS. The hydride is located *trans* to the amido ligand in the lowest-energy transition state (**TS-1a**) that leads to the (*R*)-enantiomer but is located *trans* to the pyridyl group in the lowest-energy transition state (**TS-2a**) that leads to the (*S*)-enantiomer. Error bars in **b** correspond to those in the initial rates that result from errors in the integration of peaks in the gas chromatogram.

reaction, we conducted hydroamination of *cis*-4-octene with equimolar amounts of 2-amino-6-methylpyridine and 2-aminopyridine. Whereas the reaction of 2-amino-6-methylpyridine alone afforded the hydroamination product in high yield, the reaction that contained both 2-amino-6-methylpyridine and 2-aminopyridine provided neither hydroamination product (Fig. 4c). This result implies that stronger

binding of the 2-aminopyridine than of 2-amino-6-methylpyridine inhibits the catalyst. It also implies that the methyl group of 2-amino-6-methylpyridine weakens the binding to the iridium centre, thereby allowing alkene binding and insertion.

To investigate the origin of the high levels of enantioselectivity in the hydroamination, we conducted calculations on the alkene migratory insertion using density functional theory (DFT). On the basis of the kinetic experiments, this step is probably the rate-limiting and enantio-determining step of the catalytic cycle. We calculated 12 possible isomeric transition states of migratory insertion that would lead to either enantiomer of the products with *cis*-2-butene as the model alkene. The structures of the lowest-energy transition states that lead to the major and minor enantiomers are illustrated in Fig. 4d. The two transition states of many metal-catalysed enantioselective hydrofunctionalization reactions of alkenes to form two enantiomers differ principally by the face of the alkene to which the metal is bound. In the current system, the orientation of ancillary ligands around the metal, in addition to the face of the alkene, differs greatly in the two transition states. The geometry of **TS-1a**, the transition state leading to the major enantiomer, contains meridionally oriented hydride, pyridine and amido ligands with the hydride *trans* to the amido group. By contrast, these three ligands in **TS-2a**, which is the lowest-energy transition state leading to the minor enantiomer, are arranged with the hydride *trans* to the pyridine donor. A geometry analogous to **TS-1a** that would form the opposite enantiomer by orienting the methyl groups away from the pyridine ligand (**TS-2c** and **TS-2d**; Supplementary Information Scheme S4) is higher in energy than is **TS-2a**. **TS-1a** is probably the lowest-energy transition state for several reasons. First, the Ir–N_{am} bond to the amido group, which is *trans* to a hydride in **TS-1a**, is elongated (2.32 Å), thereby leading to higher reactivity towards insertion. Second, the alkene is perpendicular to the P–Ir–P plane in **TS-1a**, whereas the alkene is almost co-planar with the P–Ir–P plane in **TS-2a**. These orientations place the substituents on the alkene in **TS-1a** farther from the phosphine ligand than those on the alkene in **TS-2a**, leading to less steric hindrance in **TS-1a** than in **TS-2a**. This analysis suggests that electronic and steric effects together impart high enantioselectivity to the hydroamination.

Our work demonstrates that the direct N–H addition of amines to unactivated internal alkenes can occur with high enantioselectivity under thermal conditions, without the need for strategies involving formal hydroamination. Despite the typically high barriers and weak thermodynamic driving force for hydroamination, the use of cationic bisphosphine-ligated iridium as the catalyst and 2-amino-6-methylpyridine as the amine led to enhancements of the rates of multiple steps within the catalytic cycle and to suppression of alkene isomerization and oxidative amination, enabling the hydroamination of unactivated internal alkenes in high yield and with high enantioselectivity. The hydroamination products can be converted to the corresponding primary amines readily with preservation of the high enantiomeric excess of the hydroamination products. These design principles should provide a starting point to address the long-standing challenge of applying hydroamination of unactivated internal alkenes to the synthesis of chiral amines and inspire advances in other asymmetric hydrofunctionalizations of internal alkenes.

Online content

Any methods, additional references, Nature Research reporting summaries, source data, extended data, supplementary information, acknowledgements, peer review information; details of author contributions and competing interests; and statements of data and code availability are available at <https://doi.org/10.1038/s41586-020-2919-z>.

1. Müller, T. E. & Beller, M. Metal-initiated amination of alkenes and alkynes. *Chem. Rev.* **98**, 675–704 (1998).

- Müller, T. E., Hultzsich, K. C., Yus, M., Foubelo, F. & Tada, M. Hydroamination: direct addition of amines to alkenes and alkynes. *Chem. Rev.* **108**, 3795–3892 (2008).
- Huang, L., Arndt, M., Gooßen, K., Heydt, H. & Gooßen, L. J. Late transition metal-catalyzed hydroamination and hydroamidation. *Chem. Rev.* **115**, 2596–2697 (2015).
- Reznichenko, A. L. & Hultzsich, K. C. in *Organic Reactions* 1–554 (Wiley, 2015).
- Gurak, J. A., Yang, K. S., Liu, Z. & Engle, K. M. Directed, regiocontrolled hydroamination of unactivated alkenes via protodepalladation. *J. Am. Chem. Soc.* **138**, 5805–5808 (2016).
- Karshtedt, D., Bell, A. T. & Tilley, T. D. Platinum-based catalysts for the hydroamination of olefins with sulfonamides and weakly basic anilines. *J. Am. Chem. Soc.* **127**, 12640–12646 (2005).
- Zhang, J., Yang, C.-G. & He, C. Gold(I)-catalyzed intra- and intermolecular hydroamination of unactivated olefins. *J. Am. Chem. Soc.* **128**, 1798–1799 (2006).
- Musacchio, A. J. et al. Catalytic intermolecular hydroaminations of unactivated olefins with secondary alkyl amines. *Science* **355**, 727–730 (2017).
- Nguyen, T. M., Manohar, N. & Nicewicz, D. A. *anti*-Markovnikov hydroamination of alkenes catalyzed by a two-component organic photoredox system: direct access to phenethylamine derivatives. *Angew. Chem. Int. Ed.* **53**, 6198–6201 (2014).
- Zhang, Z., Lee, S. D. & Widenhoefer, R. A. Intermolecular hydroamination of ethylene and 1-alkenes with cyclic ureas catalyzed by achiral and chiral gold(I) complexes. *J. Am. Chem. Soc.* **131**, 5372–5373 (2009).
- Reznichenko, A. L., Nguyen, H. N. & Hultzsich, K. C. Asymmetric intermolecular hydroamination of unactivated alkenes with simple amines. *Angew. Chem. Int. Ed.* **49**, 8984–8987 (2010).
- Pan, S., Endo, K. & Shibata, T. Ir(I)-catalyzed intermolecular regio- and enantioselective hydroamination of alkenes with heteroaromatic amines. *Org. Lett.* **14**, 780–783 (2012).
- Vanable, E. P. et al. Rhodium-catalyzed asymmetric hydroamination of allyl amines. *J. Am. Chem. Soc.* **141**, 739–742 (2019).
- Nugent, T. C. *Chiral Amine Synthesis: Methods, Developments and Applications* (Wiley VCH, 2010).
- Trowbridge, A., Walton, S. M. & Gaunt, M. J. New strategies for the transition-metal catalyzed synthesis of aliphatic amines. *Chem. Rev.* **120**, 2613–2692 (2020).
- Wang, C. & Xiao, J. in *Stereoselective Formation of Amines* (eds Li, W. & Zhang, X.) 261–282 (Springer, 2014).
- Nugent, T. C. & El-Shazly, M. Chiral amine synthesis – recent developments and trends for enamide reduction, reductive amination, and imine reduction. *Adv. Synth. Catal.* **352**, 753–819 (2010).
- Patil, M. D., Grogan, G., Bommarium, A. & Yun, H. Oxidoreductase-catalyzed synthesis of chiral amines. *ACS Catal.* **8**, 10985–11015 (2018).
- Xie, J.-H., Zhu, S.-F. & Zhou, Q.-L. Transition metal-catalyzed enantioselective hydrogenation of enamines and imines. *Chem. Rev.* **111**, 1713–1760 (2011).
- Ellman, J. A., Owens, T. D. & Tang, T. P. *N*-tert-Butanesulfinyl imines: versatile intermediates for the asymmetric synthesis of amines. *Acc. Chem. Res.* **35**, 984–995 (2002).
- You, S.-L., Zhu, X.-Z., Luo, Y.-M., Hou, X.-L. & Dai, L.-X. Highly regio- and enantioselective Pd-catalyzed allylic alkylation and amination of monosubstituted allylic acetates with novel ferrocene P,N-ligands. *J. Am. Chem. Soc.* **123**, 7471–7472 (2001).
- Ohmura, T. & Hartwig, J. F. Regio- and enantioselective allylic amination of achiral allylic esters catalyzed by an iridium–phosphoramidite complex. *J. Am. Chem. Soc.* **124**, 15164–15165 (2002).
- Löber, O., Kawatsura, M. & Hartwig, J. F. Palladium-catalyzed hydroamination of 1,3-dienes: a colorimetric assay and enantioselective additions. *J. Am. Chem. Soc.* **123**, 4366–4367 (2001).
- Adamson, N. J., Hull, E. & Malcolmson, S. J. Enantioselective intermolecular addition of aliphatic amines to acyclic dienes with a Pd–PHOX catalyst. *J. Am. Chem. Soc.* **139**, 7180–7183 (2017).
- Long, J., Wang, P., Wang, W., Li, Y. & Yin, G. Nickel/Brønsted acid-catalyzed chemo- and enantioselective intermolecular hydroamination of conjugated dienes. *iScience* **22**, 369–379 (2019).
- Tran, G., Shao, W. & Mazet, C. Ni-catalyzed enantioselective intermolecular hydroamination of branched 1,3-dienes using primary aliphatic amines. *J. Am. Chem. Soc.* **141**, 14814–14822 (2019).
- Kawatsura, M. & Hartwig, J. F. Palladium-catalyzed intermolecular hydroamination of vinylarenes using arylamines. *J. Am. Chem. Soc.* **122**, 9546–9547 (2000).
- Utsunomiya, M. & Hartwig, J. F. Intermolecular, Markovnikov hydroamination of vinylarenes with alkylamines. *J. Am. Chem. Soc.* **125**, 14286–14287 (2003).
- Yang, Y., Shi, S.-L., Niu, D., Liu, P. & Buchwald, S. L. Catalytic asymmetric hydroamination of unactivated internal olefins to aliphatic amines. *Science* **349**, 62–66 (2015).
- Gui, J. et al. Practical olefin hydroamination with nitroarenes. *Science* **348**, 886–891 (2015).
- Johns, A. M., Sakai, N., Ridder, A. & Hartwig, J. F. Direct measurement of the thermodynamics of vinylarene hydroamination. *J. Am. Chem. Soc.* **128**, 9306–9307 (2006).
- Liu, Z. & Hartwig, J. F. Mild, rhodium-catalyzed intramolecular hydroamination of unactivated terminal and internal alkenes with primary and secondary amines. *J. Am. Chem. Soc.* **130**, 1570–1571 (2008).
- Huang, J.-M., Wong, C.-M., Xu, F.-X. & Loh, T.-P. InBr₃ catalyzed intermolecular hydroamination of unactivated alkenes. *Tetrahedron Lett.* **48**, 3375–3377 (2007).
- Sevov, C. S., Zhou, J. & Hartwig, J. F. Iridium-catalyzed intermolecular hydroamination of unactivated aliphatic alkenes with amides and sulfonamides. *J. Am. Chem. Soc.* **134**, 11960–11963 (2012).
- Utsunomiya, M., Kuwano, R., Kawatsura, M. & Hartwig, J. F. Rhodium-catalyzed *anti*-Markovnikov hydroamination of vinylarenes. *J. Am. Chem. Soc.* **125**, 5608–5609 (2003).
- Pawlas, J., Nakao, Y., Kawatsura, M. & Hartwig, J. F. A general nickel-catalyzed hydroamination of 1,3-dienes by alkylamines: catalyst selection, scope, and mechanism. *J. Am. Chem. Soc.* **124**, 3669–3679 (2002).
- Casalnuovo, A. L., Calabrese, J. C. & Milstein, D. Rational design in homogeneous catalysis. Iridium(I)-catalyzed addition of aniline to norbornylene via nitrogen-hydrogen activation. *J. Am. Chem. Soc.* **110**, 6738–6744 (1988).

38. Dorta, R., Egli, P., Zürcher, F. & Togni, A. The [IrCl(diphosphine)]₂/fluoride system. Developing catalytic asymmetric olefin hydroamination. *J. Am. Chem. Soc.* **119**, 10857–10858 (1997).
39. Zhou, J. & Hartwig, J. F. Intermolecular, catalytic asymmetric hydroamination of bicyclic alkenes and dienes in high yield and enantioselectivity. *J. Am. Chem. Soc.* **130**, 12220–12221 (2008).
40. Sevov, C. S., Zhou, J. & Hartwig, J. F. Iridium-catalyzed, intermolecular hydroamination of unactivated alkenes with indoles. *J. Am. Chem. Soc.* **136**, 3200–3207 (2014).
41. Hanley, P. S. & Hartwig, J. F. Migratory insertion of alkenes into metal–oxygen and metal–nitrogen bonds. *Angew. Chem. Int. Ed.* **52**, 8510–8525 (2013).
42. Thompson, W. H. & Sears, C. T. Kinetics of oxidative addition to iridium(I) complexes. *Inorg. Chem.* **16**, 769–774 (1977).
43. Smout, V. et al. Removal of the pyridine directing group from α -substituted *N*-(pyridin-2-yl)piperidines obtained via directed Ru-catalyzed sp³ C–H functionalization. *J. Org. Chem.* **78**, 9803–9814 (2013).
44. Hanley, P. S. & Hartwig, J. F. Intermolecular migratory insertion of unactivated olefins into palladium–nitrogen bonds. Steric and electronic effects on the rate of migratory insertion. *J. Am. Chem. Soc.* **133**, 15661–15673 (2011).
45. Zhang, M., Hu, L., Lang, Y., Cao, Y. & Huang, G. Mechanism and origins of regio- and enantioselectivities of iridium-catalyzed hydroarylation of alkenyl ethers. *J. Org. Chem.* **83**, 2937–2947 (2018).
46. Xing, D., Qi, X., Marchant, D., Liu, P. & Dong, G. Branched-selective direct α -alkylation of cyclic ketones with simple alkenes. *Angew. Chem. Int. Ed.* **58**, 4366–4370 (2019).
47. Xi, Y., Butcher, T. W., Zhang, J. & Hartwig, J. F. Regioselective, asymmetric formal hydroamination of unactivated internal alkenes. *Angew. Chem. Int. Ed.* **55**, 776–780 (2016).
48. Mei, T.-S., Werner, E. W., Burckle, A. J. & Sigman, M. S. Enantioselective redox-relay oxidative heck arylations of acyclic alkenyl alcohols using boronic acids. *J. Am. Chem. Soc.* **135**, 6830–6833 (2013).
49. Morandi, B., Wickens, Z. K. & Grubbs, R. H. Regioselective Wacker oxidation of internal alkenes: rapid access to functionalized ketones facilitated by cross-metathesis. *Angew. Chem. Int. Ed.* **52**, 9751–9754 (2013).

Publisher's note Springer Nature remains neutral with regard to jurisdictional claims in published maps and institutional affiliations.

© The Author(s), under exclusive licence to Springer Nature Limited 2020

Data availability

The data that support the findings of this study are available within the article and its Supplementary Information.

Acknowledgements The enantioselective aspects of the work were supported by the National Institutes of Health under grant R35GM130387 and the catalyst development was supported by the Director, Office of Science, of the US Department of Energy under contract number DE-AC02-05CH11231. Calculations were performed at the Molecular Graphics and Computation Facility at UC Berkeley funded by the NIH (S10OD023532). We gratefully acknowledge Takasago for gifts of (S)-DTBM-SEPHOS, and H. Celik for assistance with nuclear magnetic resonance (NMR) experiments. Instruments in the College of Chemistry NMR facility are supported in part by NIH S10OD024998. We thank R. G. Bergman, B. Su and T. Butcher for discussions. Y.X. thanks Bristol-Myers Squibb for a graduate fellowship, S. Pedram for supply of NaBARF and D. Small for assistance with DFT calculations.

Author contributions Y.X. and J.F.H. conceived the project. Y.X. discovered the reaction and performed experiments and DFT calculations. S.M. performed experiments for revision. Y.X. and J.F.H. wrote the manuscript.

Competing interests The authors declare no competing interests.

Additional information

Supplementary information is available for this paper at <https://doi.org/10.1038/s41586-020-2919-z>.

Correspondence and requests for materials should be addressed to J.F.H.

Peer review information *Nature* thanks the anonymous reviewer(s) for their contribution to the peer review of this work.

Reprints and permissions information is available at <http://www.nature.com/reprints>.